


Please cite the Published Version

Li, Zhen, Meng, Zhaozong, Wu, Changcheng, Soutis, Constantinos, Chen, Zhijun, Wang, Ping and Gibson, Andrew  (2022) A new microwave cavity resonator sensor for measuring coating thickness on carbon fibre composites. NDT and E International: Independent Nondestructive Testing and Evaluation, 126. p. 102584. ISSN 0963-8695

DOI: <https://doi.org/10.1016/j.ndteint.2021.102584>

Publisher: Elsevier

Version: Accepted Version

Downloaded from: <https://e-space.mmu.ac.uk/629851/>

Usage rights:  [Creative Commons: Attribution-Noncommercial-No Derivative Works 4.0](https://creativecommons.org/licenses/by-nc-nd/4.0/)

Additional Information: This is an Accepted Manuscript of an article which appeared in NDT and E International: Independent Nondestructive Testing and Evaluation, published by Elsevier

Enquiries:

If you have questions about this document, contact openresearch@mmu.ac.uk. Please include the URL of the record in e-space. If you believe that your, or a third party's rights have been compromised through this document please see our Take Down policy (available from <https://www.mmu.ac.uk/library/using-the-library/policies-and-guidelines>)

A new microwave cavity resonator sensor for measuring coating thickness on carbon fibre composites

Zhen Li^{1*}, Zhaozong Meng², Changcheng Wu¹, Constantinos Soutis³, Zhijun Chen¹, Ping Wang¹, Andrew Gibson⁴

¹College of Automation Engineering, Nanjing University of Aeronautics and Astronautics, Nanjing, 211106, China

²School of Mechanical Engineering, Hebei University of Technology, Tianjin, 300401, China

³Aerospace Research Institute, The University of Manchester, Manchester, M13 9PL, UK

⁴Faculty of Science and Engineering, Manchester Metropolitan University, Manchester, M1 5GD, UK

*Corresponding author: zhenli@nuaa.edu.cn

Abstract:

Carbon fibre-reinforced polymer composites are widely used in modern aircraft structures for the high stiffness-to-weight ratio. An aircraft's exterior is commonly applied with coatings for minimisation of aerodynamic drag, resistance to chemicals, hydraulic fluid and ultraviolet exposure. The issues with the coatings are the possible high thickness variations due to the manual painting adopted. The existing thickness measurement methods are mostly suited to metals and cannot be well employed for in-field tests of composites. Here a new microwave cylindrical cavity resonator sensor is developed for the non-destructive thickness evaluation of coatings on composite substrates. The open cavity and conductive carbon fibre composite form a resonant system, where the presence of coating affects the surface impedance, causing changes in the resonance frequency. Applying the wall impedance perturbation and transmission line theories, an analytical model is proposed. From the measured data, a linear relationship is obtained between the resonance frequency shift and thickness change, thereby simplifying the prediction process. The insensitivity to the dielectric properties of the coating and anisotropy of the composite substrate offers convenient calibration and implementation. The new sensor can provide efficient on-site assessment of paint coatings on carbon fibre composite surfaces used in modern aircraft construction and other engineering applications.

Keywords: composites; coating thickness; cavity resonator; impedance perturbation; dielectric properties

1. Introduction

The accurate measurement of coating thickness like paint is of vital importance to the performance of aircraft since an excessive amount adds weight and increases fuel consumption. With a thinner coating though, the functions required might be compromised, such as minimisation of aerodynamic drag, resistance to chemicals and high levels of ultraviolet exposure. For a large aircraft, some manual painting is commonly conducted due to the complexity of the structures, leading to high thickness variations. Other than the conventional time-consuming weighing and destructive drilling, several non-destructive evaluation techniques have been developed. However, some cannot be readily applied to carbon fibre-reinforced polymer (CFRP) composites that are increasingly used in aircraft construction [1]. For example, optical methods (e.g., spectral interferometry) cannot be used, as the composite is not translucent. Composites are non-magnetic, and the conductivities are significantly lower than those of metals [2]. Thus, existing methods like magnetic induction and eddy current testing [3] suitable for metals cannot be used either. Intricate equipment is involved in terahertz scanning [4], so that they can only be used in a laboratory setting. Health and safety issues associated with ionising radiation in methods like gamma-ray backscattering, beta-ray transmission and X-ray fluorescence [5] need careful consideration. Ultrasonics [6] and guided waves [7] are more accurate for relatively thick coatings, but transducers and couplants are required, complicating the setup for on-site tests. Therefore, there is a need for new sensors to offer on-site assessment. Microwave testing has attracted considerable attention recently, as it has the advantages of low signal power consumption, one-sided scanning, easy setup (no need for transducers or couplants), operator friendly and no ionising radiation hazards [8,9]. This technique is more suited to dielectrics, as waves can propagate well in low-loss materials. From the signals received, the changes of the dielectric properties (also called permittivity) and/or thickness can be identified. A wide range of applications have been explored, like damage detection [10,11], medical imaging, food analysis [12,13] and security check [14]. For coating thickness measurement, some preliminary experimental research has been reported. Takeuchi et al. [15] employed a TM_{011} mode cavity resonator with a resonance frequency of approximately 15 GHz to measure coated composite panels. Very thin coatings from 50.8 μm to 203.2 μm were investigated, and calibration of different coating materials was involved. Using the fitting equation from the calibration, the average reading difference with a drilling tool (a standard wedge cut method but a destructive approach) was 5.2 %, while the accuracy by the drilling was around 10%. Hinken [16] developed a TE_{012} mode cavity and presented a calibration curve with five points for each of the three substrates measured. Only one type of plastic foil was used, and more extensive calibration was required to examine the effects of the coating

material and substrate conductivity. Zoughi et al. [17] examined dielectric layers on a woven composite substrate using an open-ended X-band (8-12 GHz) rectangular waveguide. An analytical model with the assumptions of the infinitely large waveguide flange and sample dimensions was used for the thickness extraction, where the dielectric properties of the coating sample were known. From the measurement of 1.69 mm thick garolite fiberglass-epoxy, 5.35 mm thick polyethylene (PE) and 1.28 mm thick nylon sheets, high errors with a maximum of up to 15% were obtained. System calibration was needed to shift the reference plane to the waveguide aperture, so that accurate reflection coefficients can be obtained for the solution of the inverse problem. A skilled technician and commercial open/short/load calibration kits were needed for the standard calibration procedure. The applicability for thinner samples and other types of composite substrates was not studied. Li et al. [18] developed a cavity sensor for unidirectional (UD) CFRP composite substrates. From the experiments good correlations were found between the thickness and resonance frequencies of the TM_{011} and TE_{211} modes. The estimation error was within $\pm 10\%$ for the thickness over 200 μm . From these studies, it is shown that for the open cavity resonator approach the calibration was carried out primarily using foils. By recording the resonance frequencies at different coating materials, coating thicknesses and composite substrates, calibration curves are generated. Thus, when an unknown sample is measured, its coating thickness can be estimated from the specific calibration curve corresponding to the same coating and substrate types. Therefore, the measurement accuracy is highly dependent on whether sufficient combinations of materials and thicknesses that can occur in real tests have been examined. It is concluded that the microwave methods have shown some promising results, but further work is needed to improve the measurement accuracy and ease of calibration.

The primary objective of this research is to develop a sensor that can offer accurate and convenient thickness measurement with little need of calibration. In the paper, a new open cylindrical cavity resonator sensor is presented and tested. First, the sensor design and electromagnetic simulation of the field distributions are addressed in detail. The cavity wall of the TE_{011} mode cavity is made to eliminate the degenerate TM mode (sharing the same frequency with the TE mode but exhibiting fundamentally different field distributions), so no signal interference could happen. A theoretical model is proposed to elucidate the working principle. Then, four types of dielectric foils are measured, where the effects of the coating material and thickness on the resonance frequency are thoroughly investigated and discussed. The sensitivity to the fibre direction is also examined using woven and UD CFRP plates. Finally, the performance on a copper substrate is evaluated as well. From the analytical modelling, a linear relationship is revealed between the resonance frequency

shift and the coating thickness difference. Therefore, no interpolation is involved in the inverse problem. The finding also facilitates the computation of the coefficient related, where a minimum of only two measurements are required. Thus, the calibration process is significantly simplified compared with the microwave sensors previously reported. In terms of the measurement accuracy, due to the high efficacy of the analytical model and calibration technique proposed, low errors within $\pm 4\%$ are achieved. Alternatively, an empirical coefficient value can be used as a first guess, and reasonable estimation can still be provided. It is also found that the sensor is insensitive to the substrate anisotropy, providing wide applicability.

2. Materials and methods

2.1. Materials

Four commercially available plastic films, PE, polyethylene terephthalate (PET), polyvinyl chloride (PVC) and Flame Retardant 4 (FR4) woven fiberglass-epoxy, were used to simulate the coating. The use of plastic films is common practice in the calibration and evaluation of a new coating thickness sensor. The thickness of a single layer of each material was measured by a digital micrometer, which had a resolution of 1 μm and an accuracy of $\pm 2 \mu\text{m}$. The thicknesses of PE, PET, FR4 and PVC were approximately 44 μm , 56 μm , 145 μm and 295 μm , respectively. Two 4 mm thick T300 CFRP composite substrates were used, i.e., a (0/90) plain weave and a UD laminate.

2.2. Sensor design

The sensor is made of aluminium and consists of an annular wall, which is mechanically attached to an endplate with eight socket screws. The cavity was made by a computer numerical controlled (CNC) machine. No special treatment was made on the inner surface of the cavity body. The radius of the cavity (r) is 47.5 mm, and the height (h) is 40 mm. As illustrated in Figure 1, two SubMiniature version A (SMA) connectors are mounted on the endplate. At the end of each connector a coupling loop is made, and the direction of the magnetic field generated by the loop current is the same as that of the resonant mode designated at that position. Coupling loops together with coupling probes and apertures are commonly used for the excitation of microwave cavity resonators [19].

In the transverse electric (TE) mode, the electric fields only exist in the plane transverse to the axis of the cylinder. TE_{011} is a type of TE_{nml} mode, where subscript n is the number of full-period variations along the circumference of the cylinder, m is the number of zeros of the field intensity in the radial direction, and l is the number of half-period variations along the axial direction. Hence, the electric field intensity is identical in the circumferential direction. The TE_{011} mode cavity can be

applied for several applications, such as moisture content determination of grains [20] and particle size characterisation of metallic powders [21]. However, it has not been successfully employed for the coating thickness measurement.

The resonance frequency of the TE₀₁₁ mode in an air-filled closed cylindrical cavity can be computed by

$$f_r = \frac{c}{2\pi} \sqrt{\left(\frac{p'_{01}}{r}\right)^2 + \left(\frac{\pi}{h}\right)^2} \quad (1)$$

where c is the speed of light in free space, and p'_{01} is the first root of the derivative of J_0 .

To avoid the interference of the degenerate mode, i.e., TM₁₁₁ mode, grooves are made at both the top and bottom edges of the cavity body. The groove is at an anti-node of the TM mode and a node in the TE mode. Thus, the resonance frequency of the TM mode is shifted due to the effectively larger cavity, while that of the TE mode is not affected. Numerical simulation is performed to reveal the resonant electromagnetic fields using CST[®] software. The material type of the background is set to *Normal* (i.e., vacuum), and the open boundary conditions are applied. In CST, the simulation is only performed within the bounding box of the whole structure. A boundary condition is specified for each plane (Xmin/Xmax/Ymin/Ymax/Zmin/Zmax) of the bounding box. For the open boundary condition, a perfectly matched microwave absorber material is placed at the boundary. Details about the general mathematical expressions of the boundary condition can be referred to in [22,23].

Waveguide ports are placed at the top of the connectors as seen in Figure 2 (a). The frequency domain solver is adopted, and the adaptive mesh refinement option in the solver setting is selected to generate a fine mesh. The resonance frequency computed, i.e., 5.3721 GHz, is the same as the theoretical value, confirming the sensor design. The cross-sectional views of the electric and magnetic fields are illustrated in Figures 2 (b-d), where the electric fields in the transverse plane are circumferential as would be expected. The low field intensities near the endplate indicate that slight detachment of the endplate does not significantly disturb the resonant fields. This special characteristic is useful for the measurement, where the open cavity and a conductive substrate form a closed resonant system and a dielectric coating separating the wall and the endplate only introduces a small change in the resonant responses.

2.3. Analytical model

The wall-impedance perturbation theory is adopted here, as it can characterise the impedance change when one endplate is replaced by another one while the cavity shape is kept unchanged. Let \bar{E}_a and \bar{H}_a be the electric and magnetic fields inside the original cavity. \bar{E}_b and \bar{H}_b are the electric and

magnetic fields after perturbation, respectively. ω_a and ω_b are the complex angular frequencies before and after the perturbation, respectively. For small perturbation of a cavity with a high quality factor, it is assumed that over most of the cavity $\bar{E}_a \approx \bar{E}_b$ and $\bar{H}_a \approx \bar{H}_b$, and the change of the angular frequency can be given by [24]

$$\omega_b - \omega_a \approx 2\pi(f_b - f_a) + j\pi \left(\frac{f_b}{Q_b} - \frac{f_a}{Q_a} \right) \approx j\zeta (Z_{s,b} - Z_{s,a}) \quad (2)$$

where f_a and f_b are the resonance frequencies before and after the perturbation, respectively. Q_a and Q_b are the quality factors before and after the perturbation, respectively. ζ is a positive constant that is related to the energy stored in the cavity. $Z_{s,a}$ and $Z_{s,b}$ are the surface impedances before and after the perturbation, respectively.

Here an analytical model is proposed for the coated composite. As illustrated in Figure 3, Z_s is viewed as the input impedance looking towards the coating and composite. According to the transmission line theory, Z_s can be expressed as

$$Z_s = Z_1 \frac{Z_c + Z_1 \tanh \gamma_1 t_1}{Z_1 + Z_c \tanh \gamma_1 t_1} \quad (3)$$

where t_1 is the coating thickness. Z_1 and Z_c are the wave impedances of the coating and composite substrate, respectively. The CFRP composite plate is more conductive than the coating, so Z_c is viewed considerably lower than Z_1 . For the same reason, the thickness of the composite plate is larger than the penetration depth of the signal and thus not included in the model. $\gamma_1 = \alpha_1 + j\beta_1$ is the complex propagation constant for the coating. α_1 and β_1 are the attenuation and phase constants, respectively. The value of α_1 is associated with the dielectric loss in the coating. Generally, the coating is not greatly lossy, so γ_1 is mostly imaginary, thereby $\tanh \gamma_1 t_1 \approx j \tan \beta_1 t_1$. For the small thickness of the coating under test, the value of $\tan \beta_1 t_1$ is close to $\beta_1 t_1$. Therefore, the effective surface impedance can be approximated by

$$Z_s \approx jZ_1 \beta_1 t_1 \quad (4)$$

This is similar to the case of a transmission line terminated in a short circuit. Using the definitions of Z_1 and β_1 for the TE₀₁ mode in a circular waveguide [25], the term $Z_1 \beta_1$ is equivalent to $2\pi f Z_0 / c$, where Z_0 is the impedance of free space (i.e., 376.7 Ω). Thus, the expression of Z_s becomes

$$Z_s \approx \frac{2j\pi Z_0 f}{c} t_1 \quad (5)$$

By substituting Equation (5) into Equation (2), for cases *a* and *b* mentioned, the relationship between the resonance frequency shift and coating thickness change is obtained (for small perturbation $f_a \approx f_b$)

$$f_b - f_a \approx k(t_b - t_a) \quad (6)$$

where $k = -\zeta Z_0 f_a / c$. It should be noted that in Equation (2) the imaginary part of the complex angular frequency is ignored for consistency, as by deduction no imaginary part appears on the right-hand side. The resonance frequency change is directly proportional to the thickness difference, which means that the frequency shifts downwards with increasing coating thickness. Theoretically, the frequency shift is independent of the coating and substrate types as long as the conditions of low energy dissipation and small perturbation are satisfied. Simple calibration with a minimum of only two measurements can be performed to determine the coefficient k , e.g., using two coating cases with known thicknesses. If two coating thicknesses are known in three different cases, for a third perturbation with f_c , the thickness t_c can be readily computed without knowing the k value beforehand.

$$\frac{f_c - f_a}{f_b - f_a} \approx \frac{t_c - t_a}{t_b - t_a} \quad (7)$$

2.4. Experimental setup

The setup for the coating thickness measurement is presented in Figure 4. The sensor was connected to a Fieldfox N9951A portable microwave analyser (Keysight Technologies, Santa Rosa, CA) by two flexible coaxial cables (A-info SM-SM-SFD147A, DC-18 GHz) (A-info Inc., Chengdu, China). With a MATLAB[®] programme, the transmission coefficients S_{21} were collected from the analyser and sent to a personal computer (PC) by a LAN cable. The default signal power -15 dBm (i.e., 32 μ W) was used. When the analyser was turned on, factory calibration known as *CalReady* was automatically performed at the test port connectors of the analyser. It should be noted that calibration for S-parameter measurements is not necessary here, as the resonance frequency not the magnitude is used for the thickness prediction. For the accurate measurement of the resonance frequency, a low intermediate frequency bandwidth (IFBW) of 100 Hz was applied.

Plastic film pieces with dimensions larger than the cavity aperture were cut and stacked onto the composite. The sensor was gently pressed against the film to eliminate any air gaps. A commercial eddy current technique-based coating thickness gauge (Uni-Trend Technology Co., Ltd, Dongguan, China) was also employed. This type of sensor is widely used in the industry for thin non-metallic coatings on metallic substrates. However, when the gauge was placed onto the composite plates, no reaction was observed, confirming the inapplicability.

3. Results

3.1. Numerical simulation

Here the effect of the grooves on the measurement is also studied by simulation. In the model, PET is used as the coating material with a permittivity value of $2.87-j2.74 \times 10^{-2}$ [26]. Due to the complex microstructure, the composite cannot be readily built. Hence, same as the setting adopted in [17], *Graphite* (an electrically isotropic material) from the built-in material library is used to represent the composite. As shown in Figure 5 (a), with the presence of the grooves, only one peak appears, implying that the degenerate mode is greatly suppressed. In comparison, as given in Figure 5 (b), without the grooves there is more than one resonant peak and the response is asymmetrical. The distortion is caused by the superposition of the wanted and degenerate resonances (i.e., the TE_{011} and TM_{111} modes here) in the frequency domain. Thus, the significant interference poses difficulties in the determination of the resonance frequency, demonstrating the necessity of applying the grooves. It is noted that ideally without the groove design both modes would have the same resonance frequency, while in practice slightly different resonance frequencies are generated due to inevitable small imperfections (i.e., the placement of the coupling loops) of the cavity.

For the groove case, the resonance frequency variation Δf_r with respect to the no-coating case at different layer thicknesses (t) is further computed and presented in Figure 6. A good linear relationship is shown, and the data are fitted by

$$\Delta f_r = k_1 t + k_0 \quad (8)$$

where k_0 and k_1 are the regression constants. Ideally, the intercept k_0 should be zero (i.e., no frequency shift for the uncoated case), while the value is considerably small compared with the dynamic range of the frequency shift. Therefore, both the low value of k_0 and high coefficient of determination $R^2=1$ indicate the effectiveness of Equation (6). The electric and magnetic field distributions in the coating at the maximum thickness $t=1.5$ mm are presented in Figure 7, where the patterns are same as those given in Figure 2. Hence, it is suggested that the resonant mode is not affected by the presence of the coating, further confirming the validity of the assumptions employed in the analytical modelling.

3.2. Experiments

Initially, the sensor was directly placed on the woven composite plate. The resonance frequency measured, i.e., 5.3653 GHz, is just 0.1% lower than the ideal value, though the conductivity of a metal is significantly larger than that of a composite, showing that the composite behaves more similar to metals over the microwave frequency range and a highly resonant system can still be

formed. The effect of the positioning is assessed by rotating the composite plate at different angles. As listed in Table 1, there is little variation in the resonance frequency. Three consecutive measurements were taken for each case. It is mentioned that the resonance frequencies in the three tests are the same, so the standard deviation is not provided.

PET layers on the woven composite were measured. As shown in Figure 8, the resonance frequency decreases with increasing layer number. The variation of the resonance frequency change (with respect to the no PET case, i.e., the PET-0 curve) Δf_r at different coating thicknesses are plotted in Figure 9, where the same linear trend as the simulation is observed. Thus, regression analysis is employed here. The high coefficient of determination ($R^2=0.9999$) implies good fitting. Compared with the simulation, both the k_0 and k_1 values are of the same order of magnitude, and the differences are primarily caused by the rough approximation of the electrical properties of the composite used in the simulation. In Figure 8 the quality factors for the nine PET cases are not much different, ranging from 1820 to 1850, so the high values and small changes confirm the handling of the imaginary part in Equation (2).

The performance for the other three materials was also evaluated. Similar to typical aircraft painting (0.1-0.5 mm) [27], here the maximum thickness is set below 1.5 mm, i.e., up to 30 PE layers, four PVC layers and eight FR4 layers. A wide thickness range is defined to comprehensively examine the sensor capability. As shown in Figure 10, similar linear relationships are established between the frequency shift and the coating thickness. The dielectric constants of PE, PET, PVC and FR4 are approximately 2.25, 2.87, 2.84 and 4.32, respectively [28]. It is seen that the value of k_1 is larger for a material at a higher dielectric constant. Specifically, from PE to FR4 the dielectric constant is increased by 92%, while the value of k_1 is increased by only 8%. The values of k_1 would be the same if the most significant digit is kept, demonstrating good agreement with the theoretical modelling. It is noted that in practice the coating materials do not significantly vary. Hence, the insensitivity of the measurement to the coating material is confirmed.

Eight more FR4 layers (i.e., 9-16 layers in total) were evaluated as well. The linear equation obtained is applied for the resonance frequency estimation. As given in Table 2, the discrepancy between the predicted and measured values increases with increasing thickness. At $t=1305 \mu\text{m}$ the difference is -0.6% and even in the thickest case examined the error is within $\pm 5\%$, showing the sensor's applicability to thicker coatings.

4. Discussions

4.1. Effect of the conductivity anisotropy of the substrate

The UD composite plate is more conductive along the fibres than perpendicular to the fibres, showing stronger anisotropy than the woven composite. Thus, the variation of the resonance frequency is studied at different PET layer thicknesses and rotation angles of the composite plate. As presented in Figure 11, the resonance frequencies for the seven rotation angles are closely distributed. For example, at $t=560\ \mu\text{m}$, the difference between the highest and lowest points is within $\pm 0.01\%$. Linear fitting is also carried out on the frequency changes, and the coefficients obtained are given in Table 3. Same as the woven composite case, better agreement is seen in k_1 (-0.0580 ± 0.0002), which is the same as that given in the woven composite case (Figure 6). The values of k_0 can also be considered negligible.

4.2. Thickness estimation using the two-case calibration technique

Here the experimental data of PE, PET, PVC and FR4 on the woven composite plate are considered, and the thickness is estimated from the resonance frequency shift with respect to the composite only case using Equation (6). For each material, the cases with the two smallest thicknesses are used for the calculation of the k value. As shown in Figure 12, the resultant prediction errors are well within $\pm 4\%$, and the mean of the absolute error is approximately 1.36%. The estimation technique is also applied to the cases with PET on copper, and the resonance frequencies obtained are listed in Table 4. The resonance frequency for the copper only case is 5.3705 GHz. The k value calculated is -0.06, which is close to the average value of the k_1 results for the woven composite case shown in Figure 6 and Figure 7. The corresponding estimation errors are within $\pm 3\%$. The high accuracy given by the analytical model can be explained by the fact that the conductivity of copper is significantly higher than that of the composite and the assumptions used in the modelling are still valid. In the tests 401 frequency sampling points over a span of 20 MHz were used, so the resolution of the thickness estimation is around $0.83\ \mu\text{m}$.

5. Concluding remarks

A novel microwave cavity resonator sensor has been developed for the thickness measurement of coatings on CFRP composite plates. The presence of the coating perturbs the surface impedance of the resonant system formed by the sensor and the composite, producing changes in the resonance frequency. From the resonance frequency shift, the coating thickness can be determined. With the special design of grooves in the cavity body, no parasitic mode occurs. Owing to the symmetric electric field distribution of the resonant mode chosen, the sensor is shown insensitive to the

anisotropy of the composite substrate, thereby facilitating easy positioning. An analytical model has shown that linear correlation can be established between the resonance frequency shift and thickness change. From the simulation of the thickness measurement, it has been found that the possible signal interference caused by the degenerate mode can be well eliminated by the groove design, and the linear relationship is also found. The findings are in good agreement with the experimental results of four plastic films, i.e., PE, PET, PVC and FR4. In addition, it has been shown that the rate of the resonance frequency shift is not highly dependent on the coating material, confirming the accuracy of the model proposed. Reasonable results can still be offered at a coating thickness of approximately 2 mm. Using resonance frequencies of two reference cases as a simple form of calibration, the coating thickness can be readily estimated, and low errors within $\pm 4\%$ have been offered, demonstrating the advantage of easy implementation. The sensor has also been applied to metallic substrates, and errors within $\pm 3\%$ have been achieved. It is suggested that an empirical coefficient value (i.e., $k=-0.06$) can be used for the prediction as a first guess. In near future work, curved surfaces will be examined, where the probe aperture can be designed with the same curvature for fitting. Robotic arms can be used to speed up the scanning process. In addition, a low-cost microwave source with a short frequency bandwidth will be developed to replace the commercial network analyser. For further modelling, improvement of the analytical model will also be attempted to cope better with a more realistic multi-coating case.

Acknowledgements

This work was financially supported by the Natural Science Foundation of Jiangsu Province (Grant No. BK20200427), the Shuangchuang Project of Jiangsu Province (Grant No. KFR20020), the Fundamental Research Funds for the Central Universities (Grant No. NS2020019) and the National Natural Science Foundation of China (Grant No. 52105552). The first author gratefully acknowledges Prof. Yang Ju (Nagoya University, Japan) for many useful discussions. Special thanks to Dr. Fei Fei for assistance in the experiments.

References

- [1] Soutis C. Carbon fiber reinforced plastics in aircraft construction. *Mater Sci Eng A* 2005;412:171–6. doi:10.1016/j.msea.2005.08.064.
- [2] Li Z, Haigh A, Soutis C, Gibson A. X-band microwave characterisation and analysis of carbon fibre-reinforced polymer composites. *Compos Struct* 2019;208:224–32. doi:10.1016/j.compstruct.2018.09.099.

- [3] Yin W, Peyton AJ. Thickness measurement of non-magnetic plates using multi-frequency eddy current sensors. *NDT E Int* 2007;40:43–8. doi:10.1016/j.ndteint.2006.07.009.
- [4] Im K-HH, Yang I-YY, Kim S-KK, Jung J-AA, Cho Y-TT, Woo Y-DD. Terahertz scanning techniques for paint thickness on CFRP composite solid laminates. *J Mech Sci Technol* 2016;30:4413–6. doi:10.1007/s12206-016-0903-1.
- [5] de Almeida E, Melquiades FL, Marques JPR, Marguá E, de Carvalho HWP. Determination of the polymeric thin film thickness by energy dispersive X-ray fluorescence and multivariate analysis. *Spectrochim Acta Part B At Spectrosc* 2020;167:105818. doi:10.1016/j.sab.2020.105818.
- [6] Pant B, Skinner SR, Steck JE. Paint Thickness Measurement Using Acoustic Interference. *IEEE Trans Instrum Meas* 2006;55:1720–4. doi:10.1109/TIM.2006.880294.
- [7] Ostiguy P-C, Quaegebeur N, Masson P. Non-destructive evaluation of coating thickness using guided waves. *NDT E Int* 2015;76:17–25. doi:10.1016/j.ndteint.2015.08.004.
- [8] Li Z, Wang P, Haigh A, Soutis C, Gibson A. Review of microwave techniques used in the manufacture and fault detection of aircraft composites. *Aeronaut J* 2021;125:151–79. doi:10.1017/aer.2020.91.
- [9] Li Z, Haigh A, Soutis C, Gibson A. Principles and Applications of Microwave Testing for Woven and Non-Woven Carbon Fibre-Reinforced Polymer Composites: a Topical Review. *Appl Compos Mater* 2018;25:965–82. doi:10.1007/s10443-018-9733-x.
- [10] Li Z, Haigh A, Soutis C, Gibson A, Sloan R. Microwaves Sensor for Wind Turbine Blade Inspection. *Appl Compos Mater* 2017;24:495–512. doi:10.1007/s10443-016-9545-9.
- [11] Li Z, Wang T, Haigh A, Meng Z, Wang P. Non-contact detection of impact damage in carbon fibre composites using a complementary split-ring resonator sensor. *J Electr Eng* 2019;70:489–93. doi:10.2478/jee-2019-0083.
- [12] Li Z, Haigh A, Wang P, Soutis C, Gibson A. Characterisation and analysis of alcohol in baijiu with a microwave cavity resonator. *LWT* 2021;141:110849. doi:10.1016/j.lwt.2021.110849.
- [13] Li Z, Haigh A, Wang P, Soutis C, Gibson A. Dielectric spectroscopy of Baijiu over 2–20 GHz using an open-ended coaxial probe. *J Food Sci* 2021;86:2513–24. doi:10.1111/1750-3841.15738.
- [14] Kapilevich BY, Harmer SW, Bowering NJ. *Non-Imaging Microwave and Millimetre-Wave Sensors for Concealed Object Detection*. New York: CRC Press; 2014.
- [15] Takeuchi JS, Perque M, Anderson P, Sergoyan EG. Microwave paint thickness sensor. US 7898265, 2011.

- [16] Hinken J. Device for measuring coating thickness. US 9395172, 2016.
- [17] Zoughi R, Gallion JR, Ghasr MT. Accurate Microwave Measurement of Coating Thickness on Carbon Composite Substrates. *IEEE Trans Instrum Meas* 2016;65:951–3. doi:10.1109/TIM.2016.2526698.
- [18] Li Z, Meng Z, Soutis C, Haigh A, Wang P, Gibson A. Bimodal Microwave Method for Thickness Estimation of Surface Coatings on Polymer Composites. *Adv Eng Mater* 2021:2100494. doi:10.1002/adem.202100494.
- [19] Nyfors EG. Cylindrical microwave resonator sensors for measuring materials under flow. Helsinki University of Technology, 2000.
- [20] Gibson AAP, Ng SK, Noh BBM, Chua HS, Haigh AD, Parkinson G, et al. An overview of microwave techniques for the efficient measurement of food materials. *Food Manuf Effic* 2008;2:35–43. doi:10.1616/1750-2683.0026.
- [21] Clark N, Jones N, Setchi R, Porch A. Particle size characterisation of metals powders for Additive Manufacturing using a microwave sensor. *Powder Technol* 2018;327:536–43. doi:10.1016/j.powtec.2017.11.042.
- [22] Booton RC. *Computational Methods for Electromagnetics and Microwaves*. John Wiley&Sons; 1992.
- [23] Qiushi Chen, Konrad A. A review of finite element open boundary techniques for static and quasi-static electromagnetic field problems. *IEEE Trans Magn* 1997;33:663–76. doi:10.1109/20.560095.
- [24] Donovan S, Klein O, Dressel M, Holczer K, Grüner G. Microwave cavity perturbation technique: Part II: Experimental scheme. *Int J Infrared Millimeter Waves* 1993;14:2459–87. doi:10.1007/BF02086217.
- [25] Pozar DM. *Microwave Engineering*. Fourth edi. New York: John Wiley & Sons; 2012. doi:10.1007/s13398-014-0173-7.2.
- [26] Zechmeister J, Lacik J. Complex Relative Permittivity Measurement of Selected 3D-Printed Materials up to 10 GHz. 2019 Conf. Microw. Tech., IEEE; 2019, p. 1–4. doi:10.1109/COMITE.2019.8733590.
- [27] Moupfouma F. Aircraft Structure Paint Thickness and Lightning Swept Stroke Damages. *SAE Int J Aerosp* 2013;6:2013-01–2135. doi:10.4271/2013-01-2135.
- [28] Hippel AR Von. *Dielectric materials and applications*. 2nd ed. New York: Artech House; 1995.

Tables

Table 1 Variation of the resonance frequency due to the rotation of the woven CFRP composite plate

Rotation angle (°)	0	15	30	45	60	75	90
Resonance frequency f_r (GHz)	5.3653	5.3655	5.3655	5.3653	5.3648	5.3643	5.3643

Table 2 Comparison between the resonance frequencies measured and estimated using Equation (8) for thicker FR4 foils

Total thickness (μm)	1305	1450	1595	1740	1885	2030	2175	2320
Δf_r measured (MHz)	-82.6	-92.4	-102.3	-112.0	-122.1	-132.3	-142.6	-153.2
Δf_r estimated (MHz)	-82.1	-91.3	-100.4	-109.5	-118.6	-127.7	-136.8	-145.9
Error (%)	-0.57	-1.26	-1.88	-2.29	-2.87	-3.50	-4.08	-4.76

Table 3 Regression constants and coefficients of determination (R^2) for the fitting of the resonance frequencies in the unidirectional composite substrate case

Rotation angle (°)	0	15	30	45	60	75	90
k_1	-0.0580	-0.0578	-0.0582	-0.0582	-0.0581	-0.0578	-0.0579
k_0	-0.2380	-0.2926	-0.0822	0.2054	0.6565	0.4975	0.6592
R^2	0.9999	0.9999	0.9999	0.9999	0.9999	0.9999	0.9999

Table 4 Accuracy of the thickness measurement of PET layers on copper

Number of layers	2	4	6	8	10	15	20
Total thickness (μm)	112	224	336	448	560	840	1120
Resonance frequency (GHz)	5.3637	5.3574	5.3509	5.3443	5.3377	5.3215	5.3054
Estimated thickness (μm)	114.44	219.72	328.06	437.22	547.22	817.22	1086.39
Error (%)	2.18	-1.91	-2.36	-2.41	-2.28	-2.71	-3.00

Figure captions

Figure 1 Schematic diagram of the cross section of the cavity resonator sensor developed for coating thickness measurement (not to scale)

Figure 2 Simulation of the sensor closed by an aluminium endplate: (a) simulation model and transmission coefficient (S_{21}) curve; (b) electric fields in the transverse plane; (c) electric fields in the y - z plane (pointing to the paper on the left-hand side and pointing out of the paper on the right-hand side); (d) magnetic fields in the y - z plane

Figure 3 Geometry for the modelling of the coating thickness measurement using an open cavity resonator

Figure 4 Schematic diagram of the setup for coating thickness measurement with the new microwave resonator sensor

Figure 5 Simulation of the resonant responses at varied PET layer thicknesses on a graphite sheet: (a) sensor with grooves; (b) sensor without grooves

Figure 6 Resonance frequency shifts simulated at different PET layer thicknesses

Figure 7 Simulation results of the field distributions inside the 1.5 mm thick PET layer: (a) electric field (relatively low field intensity out of the cavity); (b) magnetic field

Figure 8 Signal responses for PET layers on a woven CFRP composite substrate (here PET-6 denotes six PET layers)

Figure 9 Variation of the resonance frequency shift with respect to the total thickness of the stacked PET layers on the woven CFRP composite

Figure 10 Shift of the resonance frequency due to increased thickness for PE, PVC and FR4 layers

Figure 11 Variation of the resonance frequency at different PET layer thicknesses and rotation angles of the unidirectional composite plate

Figure 12 Thickness estimation errors for PE, PET, PVC and FR4 using the two-case calibration technique